JOURNAL OF CATALYSIS **162,** 327–338 (1996)
ARTICLE NO. 0290

A Kinetic Study of *n*-Heptane Catalytic Cracking over a Commercial Y-Type Zeolite under Supercritical and Subcritical Conditions

Zissis Dardas, Murat G. Süer, Yi. H. Ma, and William R. Moser[1]

Department of Chemical Engineering, Worcester Polytechnic Institute, Worcester, Massachussetts 01609

Received November 14, 1995; revised April 10, 1996; accepted April 15, 1996

Heptane catalytic cracking over a commercial Y-type zeolite (Promoted Octacat) was studied at 475°C under subcritical and supercritical hydrocarbon conditions. Kinetic measurements showed that the activity of the catalyst was substantially higher during supercritical cracking, suggesting stabilization of the catalyst toward rapid deactivation. A mechanism based on kinetic and *in situ* cylindrical internal reflectance FTIR (CIR-FTIR) results was developed to explain the performance of the catalyst under supercritical conditions. The dense supercritical reaction medium, well known for its enhanced solubilization capabilities, continuously removes the newly formed coke through solubilization from the zeolite supercages, pore mouths, and the external surface. This results in a higher number of available active sites to perform catalytic cracking and in lower pore diffusion limitations due to the avoidance of pore blockage. The significantly higher yields of the olefinic and paraffinic reaction products and the higher paraffin/olefin ratios under supercritical cracking conditions are in agreement with the above mechanism. Finally, it was shown that a partial regeneration of a moderately deactivated cracking catalyst is possible by the supercritical reaction medium. Reactivation of a severely deactivated catalyst could not be achieved.

INTRODUCTION

A fluid is said to be "supercritical" when its temperature and pressure are above the temperature and pressure at the critical point. Supercritical fluids offer unique advantages over gas-phase media for numerous catalytic reactions. The liquid-like density enhances their solubilization efficiency while the gas-like viscosity, surface tension, and diffusivity enable easy penetration into the pores of a catalyst for extraction of nonvolatile compounds in the pores (1). These properties should be beneficial for catalytic cracking reactions where the zeolite pores are rapidly filled with coke.

Savage *et al.* (2) gave an excellent comprehensive review on fundamentals and applications of reactions under supercritical conditions, summarizing all the existing literature in these subjects up to 1995. For heterogeneous catalysis, extended studies in olefin isomerization (3–11) and Fischer–Tropsch synthesis (1, 12) under supercritical reaction media have been reported. Tiltscher *et al.* (3–5) for the first time demonstrated the potential applications of supercritical fluids (SCF) for heterogeneous catalytic reactions by comparing results for identical reaction conditions in the gas, liquid, and SCF phases. The reaction they mainly studied was 1-hexene isomerization on a low-activity, macroporous α-Al_2O_3 and they showed that deactivation of the catalyst occurred during the gas-phase reaction due to the deposition of hexene oligomers on the catalytically active sites. When they performed the reaction at the same temperature but above the critical pressure, deposition of these oligomers was prevented and the catalyst activity was maintained. They concluded that the supercritical reaction medium had the ability to perform *in situ* extraction of coke precursors.

Subramaniam and co-workers (6–11) greatly extended this work by investigating this reaction over a high-activity, microporous, industrial Pt/γ-Al_2O_3 catalyst. In sharp contrast to the activity maintenance observed by Tiltscher and co-workers in the macroporous catalyst, the microporous catalyst used by Saim and Subramaniam (7, 8) deactivated even under supercritical conditions. Modeling the coke formation and sequential *in situ* coke extraction (9) for the process showed that there is an optimum supercritical pressure (i.e., reaction mixture density) at which catalyst performance is maximized. For example, at lower than optimum densities, the catalyst undergoes deactivation due to the lack of coke extraction while at higher than optimum densities the catalyst activity decreases due to pore-diffusion limitations in the superdense, liquid-like reaction mixture. Ginosar and Subramaniam (11) confirmed these qualitative predictions by investigating 1-hexene isomerization at reaction mixture densities ranging from gas-like (subcritical) to liquid-like densities at very high pressures.

Manos and Hoffman (13), performing disproportionation experiments with supercritical ethyl benzene and benzene over an USHY zeolite, showed that only coke precursors can be dissolved and therefore, complete coke removal by supercritical fluids is impossible. They also demonstrated

[1] To whom correspondence should be addressed. E-mail address: wmoser@wpi.edu.

0021-9517/96 $18.00

that under supercritical conditions less coke was deposited on the catalyst and therefore, the catalyst deactivation was reduced. Coke solubilization by the supercritical fluid was also verified by the color of the fluid in the condenser; the normally colorless liquid become yellowish-brown indicating the presence of polyaromatics.

The gas-like diffusivity and the liquid-like solubility were the major factors that motivated the research into conducting Fischer–Tropsch synthesis (FTS) reaction in a supercritical phase (1, 12). Lang *et al.* (1) and Yokota and Fujimoto (12) investigated the Fischer–Tropsch synthesis in the presence of a supercritical solvent (propane and *n*-hexane, respectively). While the catalyst activity and hydrocarbon product distribution were similar to those obtained under baseline conditions (subcritical pressures), higher selectivities of 1-olefins were obtained in the presence of supercritical solvent. They attributed this effect to the higher diffusivities and desorption rates of the olefins due to the *in situ* extraction of high-molecular-weight products (wax) from the pores by the supercritical solvent. The supercritical phase reactions also reduced the production of undesired products.

Numerous studies of *n*-heptane cracking over Y-type zeolites under ambient pressures have been reported in the literature (14–21). However, to our knowledge there are no studies on supercritical catalytic cracking of hydrocarbons. The supercritical reactions discussed before (isomerization, Fischer–Tropsch synthesis) were performed at temperatures around the critical temperatures (relatively low temperatures, i.e., $1 < T/T_c < 1.1$), where significant changes in the fluid density occurs with changes of the pressure near the critical pressure (22). At catalytic cracking temperatures (above 450°C), very high pressures (above 170 bar) are demanded for the supercritical fluid to reach liquid-like densities (22) (i.e., $\rho_R = \rho/\rho_c > 1$). Therefore, applications of supercritical fluids for solubilization of the coke molecules from the zeolite micropores during catalytic cracking may seem unattractive. However, studies performed at United Technologies on processing jet fuels over silicoaluminophosphates (SAPO) and other metal-supported catalysts under high pressures and temperatures showed a high stability of these catalysts toward rapid deactivation (23). On the other hand, *in situ* CIR-FTIR studies perfomed in our laboratory (24) on heptane cracking over a commercial Y-type zeolite (promoted Octacat) at 475°C clearly demonstrated that the density of heptane within the zeolite micropores was significantly higher than that computed by the Peng–Robinson equation of state (25). Thus, pressures significantly lower than those predicted by the equation of state are required for the supercritical reactant to reach liquid-like densities.

The above observations suggest that supercritical hydrocarbons might be attractive for high-temperature reactions within microporous materials (like hydrocarbon catalytic cracking over zeolites), due to the densification effect of the micropores. Therefore, the major objective of this study was to understand the effects of supercritical conditions on *n*-heptane catalytic cracking using kinetic measurements, which were coupled with *in situ* CIR-FTIR results. By the noted differences in the conversion levels, degree of deactivation, apparent rate constants under steady-state reaction conditions, and product selectivities, conclusions regarding the beneficial effect of the supercritical state on the deactivation behavior of the catalyst were developed.

EXPERIMENTAL

A detailed description of the experimental apparatus and plug flow microreactor together with technical information about the zeolite catalyst (promoted Octacat) was previously given (24). All catalytic cracking experiments were carried out at 475°C and variable pressures in the subcritical and supercritical regime. The pressure of the system was increased using a by-pass line; when the desired system pressure was obtained, the liquid heptane stream was then switched so that it flowed into the reactor. Approximately 20 s were required for the reactor to reach the desired pressure. Minimization of the reactor fillup time is very critical since a significant portion of the catalyst activity is lost due to the buildup of unextractable coke in the catalyst pores during the subcritical phase of reactor fillup.

The catalyst samples were calcined in air at 450°C for over 8 h prior to each cracking experiment. Fresh catalyst (1.60 g) was used in each experiment. Blank experiments were also performed to determine the extent of thermal cracking under these reaction conditions. Heat-traced lines carried the reactor effluent to a Perkin-Elmer Sigma 2000 gas chromatograph for product analysis and identification. The products were separated by a Chromapak 10 ft × 0.125 in. column of *n*-octane over 80/100 mesh Poracil C (which separates all reaction products except hydrogen) and analyzed by a flame ionization detector (FID). Peak integration was performed using the Grams386 Galactic software.

CH_4 was used as an internal standard for kinetic measurements (reaction rate, conversion, product selectivities and yields). Since methane is also a minor reaction product, an internal standard flow rate of at least 20 times higher than the methane production rate was continuously mixed with the reactor effluent. Furthermore, two extra measurements without internal standard were taken under the reaction steady-state conditions to correct the methane internal standard peak.

Steady-state reaction rate data for different runs under the same reaction conditions are shown in Table 1. These data illustrate that the observed significant differences between supercritical and subcritical reaction conditions are statistically significant, i.e., well outside the experimental

TABLE 1

Steady-State Reaction Rates (in Moles/(Hour Gram of Catalyst)) for Different Runs for *n*-Heptane Catalytic Cracking over Promoted Octacat at 475°C (SD, standard deviation)

P/P_c	Run 1	Run 2	Run 3	Average	SD
1.50	0.106	0.109	0.104	0.106	0.0025
1.03	0.065	0.063	0.068	0.065	0.0026
0.62	0.022	0.027	0.024	0.024	0.0025

error in these measurements and therefore, they should only be attributed to the supercritical effect.

RESULTS AND DISCUSSION

Activity Measurements under Supercritical and Subcritical Reaction Conditions

Table 2 presents the reduced densities ($\rho_R = \rho/\rho_c$) for the reaction mixture within the zeolite micropores under different operating pressures, evaluated using the Peng–Robinson equation of state (which assumes no condensation effect in the zeolite micropores) and estimated from a detailed analysis (26) of the *in situ* CIR-IR spectra of the C–H stretching modes of the reaction hydrocarbon mixture. A complete analysis of the formation of a denser fluid phase within the zeolite micropores will be given later on in a separate publication. The critical conditions for heptane are 267°C and 2750 kPa (22). Since the hydrocarbon density significantly changes with pressure, especially in the supercritical regime, the heptane inlet flow rate in each experiment was properly adjusted so that the same residence time of 0.90 s could be obtained for all different operating pressures.

Table 3 shows the reaction rates per gram of catalyst for the *n*-heptane catalytic cracking while Fig. 1 presents the corresponding catalytic activities (ratio of the reaction rate at time t to that at time $t=0$) at different times-on-stream for two subcritical (615 kPa, $P/P_c = 0.25$, $\rho_R = 0.09$ and 1715 kPa, $P/P_c = 0.62$, $\rho_R = 0.17$) and two supercritical (2850 kPa, i.e., $P/P_c = 1.03$, $\rho_R = 0.33$ and 4110 kPa, i.e., $P/P_c = 1.50$, $\rho_R = 1.40$) processing conditions. The initial rate ($t=0$) for each experiment was estimated by extrapolation of the early time heptane conversion function for $t=0$ min. The activity data (or the conversions) are most useful for the evaluation of the performance of the catalyst under operating conditions different than the reaction rates, because, as we discussed before, these experiments were run while maintaining the same residence time. Since the fluid densities are significantly higher under high pressures, the heptane inlet flow rate for the different runs was properly increased with pressure to keep the fluid residence time constant and therefore, the reaction rates were substantially higher for the supercritical experiments. The following observations were made from this figure: The deactivation of

TABLE 2

Operating Conditions for *n*-Heptane Catalytic Cracking at 475°C

P/P_c	ρ_R (empty reactor)[a]	ρ_R (pores)[b]
0.25	0.050	0.09
0.62	0.125	0.17
1.03	0.217	0.33
1.50	0.330	1.40
2.00	0.470	1.90

[a] Evaluated using Peng–Robinson equation of state (25).
[b] Estimated using *in situ* CIR-IR results.

TABLE 3

Reaction Rates (in Moles/(Hour Gram of Catalyst)) at Different Times-on-Stream for Supercritical ($P/P_c = 1.50$, $\rho_R = 1.40$), Near-Supercritical ($P/P_c = 1.03$, $\rho_R = 0.33$), and Subcritical ($P/P_c = 0.62$, $\rho_R = 0.17$, and $P/P_c = 0.25$, $\rho_R = 0.09$) *n*-Heptane Catalytic Cracking at 475°C

Time (min)	$P/P_c = 1.50$	$P/P_c = 1.03$	$P/P_c = 0.62$	$P/P_c = 0.25$
10	0.211	0.194	0.110	
45	0.173	0.135	0.061	0.007
105	0.145	0.084	0.029	
135		0.075	0.026	
180	0.108	0.069	0.024	
200		0.065	0.023	
240	0.105	0.063	0.022	
280	0.106	0.064	0.021	
300	0.106	0.064	0.022	

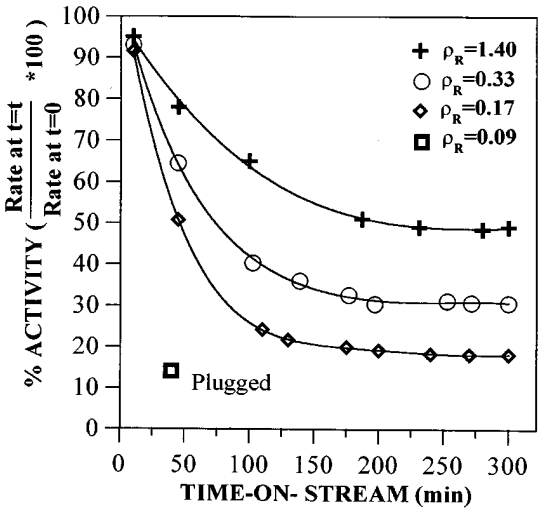

FIG. 1. Catalytic activity at different times-on-stream for subcritical (685 kPa, $\rho_R = 0.09$ and 1715 kPa, $\rho_R = 0.17$), near-supercritical (2850 kPa, $\rho_R = 0.33$) and supercritical (4110 kPa, $\rho_R = 1.40$) *n*-heptane cracking over promoted Octacat at 475°C.

the zeolite followed the same exponential decay function in all experiments, i.e., the cracking activity decreased at a moderate rate with time-on-stream for the first 100 min. The slope of the deactivation curve for the early reaction times, however, increased significantly as the operating pressure decreased, especially for subcritical conditions, indicating a higher deactivation rate under these conditions. For $P/P_c = 1.50$ ($\rho_R = 1.40$) the catalyst deactivated slowly whereas at low subcritical pressures the catalyst lost its activity rapidly. It is also noteworthy that the high-pressure supercritical experiment ($P/P_c = 1.50$, $\rho_R = 1.40$) rapidly reached a steady state and experienced no further deactivation over 5 h. At 685 kPa ($P/P_c = 0.25$, $\rho_R = 0.09$) the activity dramatically decreased during the first 40 min, which resulted in plugging of the reactor by the rapid coke formation after 60 min of time-on-stream (no data could be collected for this low pressure after 40 min of time-on-stream). The most important aspect, however, was that the steady-state activity for supercritical heptane cracking at 4110 kPa ($\rho_R = 1.40$) was significantly higher at all reaction times than for subcritical heptane. A lower pressure supercritical cracking experiment ($P/P_c = 1.03$, $\rho_R = 0.33$) showed an intermediate behavior. All these observations clearly suggest that the zeolite maintains a substantially higher steady-state catalytic activity during *n*-heptane cracking under supercritical conditions.

Figures 2 and 3 plot the steady-state heptane conversion and the catalyst activity loss, respectively, for two subcritical and two supercritical cracking experiments. The steady-state conversion for $P/P_c = 0.25$ ($\rho_R = 0.09$) has been estimated also by extrapolation, assuming the same functional decay form with that for $P/P_c = 0.62$ ($\rho_R = 0.17$). As this figure illustrates, the activity decreased as the hydrocarbon pressure decreased but it declined sharply for subcritical pressures (for $P/P_c < 0.62$). The catalyst lost 48% of its initial activity after 5 h of supercritical *n*-heptane cracking at $P/P_c = 1.50$ ($\rho_R = 1.40$) and 80% at $P/P_c = 0.62$ ($\rho_R = 0.17$) but it lost 85% of its initial activity after 40 min under the lower hydrocarbon pressure ($P/P_c = 0.25$, $\rho_R = 0.09$). These results are in excellent agreement with the results of the *in situ* monitoring of these processes by cylindrical internal reflectance FTIR (CIR-FTIR) (26). The CIR-FTIR spectra, taken under reaction conditions, showed that at steady state, for $P/P_c = 0.62$, the catalyst lost 57% of the initial Brønsted acid sites (the centers for catalytic activity) while for $P/P_c = 1.50$ it lost only 27% of them. On the other hand, from the IR analysis 68% and 8%, respectively, of the outer surface terminal silanols were consumed. Coke formation is expected to account for the consumption of the active sites.

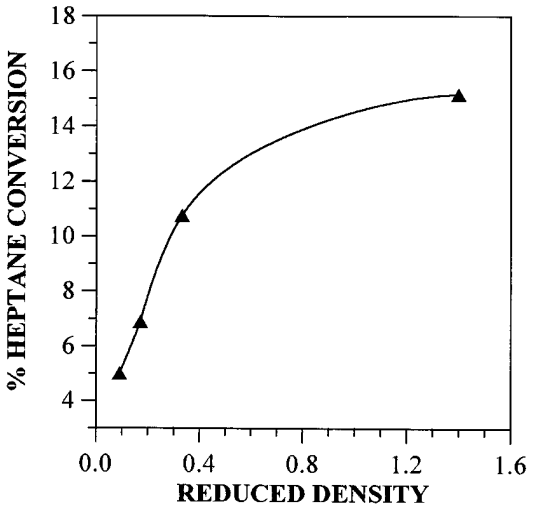

FIG. 2. Percentage heptane conversion under steady-state reaction conditions ($t = 5$ h) for different values of reduced fluid density (subcritical and supercritical conditions) during *n*-heptane cracking over promoted Octacat at 475°C.

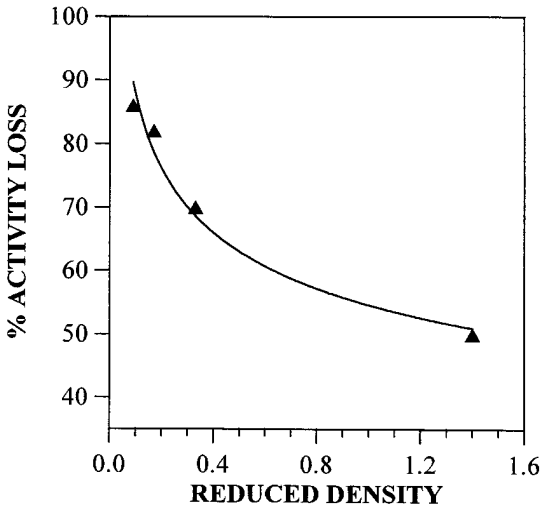

FIG. 3. Percentage activity loss under steady-state reaction conditions ($t = 5$ h) as compared to activity after 10 min for different values of reduced fluid density (subcritical and supercritical conditions) during *n*-heptane cracking over promoted Octacat at 475°C.

Modes of Catalyst Deactivation under Subcritical and Supercritical Reaction Conditions

According to Magnoux *et al.* (21), who studied the *n*-heptane cracking at 450°C over USHY zeolites under very low partial pressure (30 kPa), initially polyaromatics with alkyl groups are rapidly formed on the strong acid sites from oligomerization and condensation reactions of the olefinic products. As soon as they attain a certain size (more than three aromatic rings) their migration becomes very slow and they partially or completely obstruct the pore entry of the supercages limiting or preventing access of the reactant to the acid sites. The degree of reactant obstruction and the number of consumed Brønsted active sites depend on the location of coke in the supercages. The location depends on whether the molecule is adsorbed or not (21).

According to this model the coke molecules grow slowly in size occupying several supercages while those located on acid sites near the external surface spread over the external surface from the pore mouths. Coke molecules can also form directly on the external acid sites (19). Strong evidence for coke formation on the external surface was obtained from the infrared analysis (26) by the observation that the terminal silanols in the zeolite were substantially consumed under subcritical cracking conditions.

On the other hand, it is well known that supercritical fluids have an enhanced solubilization efficiency (27–29). Compounds that are largely insoluble in a liquid even at high temperatures can become soluble in a fluid under supercritical conditions. Solubilization studies of phenanthrene used to simulate coke precursors in a wide variety of supercritical hydrocarbons in our laboratory by the CIR-IR technique clearly showed greatly increased supercritical solubilization (30). It has been reported that this phenomenon starts for reduced densities (ρ/ρ_c) around 0.75 (28) and becomes dominant near the critical point. After the critical density is reached, the fluid solvent power significantly increases even with small increases in pressure, because (i) the high compressibility in the supercritical regime induces large changes in the density of the fluid (1, 28), and (ii) the interactions between the supercritical solvent and the dissolved molecule became more intense (30).

Saim and Subramaniam (7, 8) demonstrated that although the coke laydown significantly decreased under pressures deeply into the supercritical regime (i.e., reaction mixture reduced densities between 1.80 and 2.20), 1-hexene isomerization rates over an industrial $Pt/\gamma\text{-}Al_2O_3$ catalyst were lower and deactivation rates were higher due to pore diffusion limitations in the liquid-like reaction mixture. They observed the highest isomerization rate for ρ_R between 1.20 and 1.30 and they concluded that near-critical reaction mixtures provide the optimum combination of solvent and transport properties for maximizing the isomerization rates and for minimizing catalyst deactivation rates. On the basis of this analysis, we conclude that for our catalytic cracking experiments the supercritical reaction mixture density ($\rho_R = 1.40$) corresponding to $P/P_c = 1.50$ falls within the optimum density regime for activity maintenance. Under this pressure, the coke extraction rate within the pores was high while the molecular pore diffusion limitations of reactant and products in the reaction medium were relatively low.

We postulate the following model for the deactivation behavior of the zeolite under subcritical and supercritical conditions: For pressures well into the subcritical regime (low P/P_c and therefore low ρ_R values) the solubilization efficiency for the gaseous heptane phase is very low. Therefore, the severe catalyst deactivation, which we observed under low operating pressures, is due to (i) a rapid formation of coke molecules on the strongly acidic Brønsted acid sites and, therefore, consumption of the active sites, (ii) obstruction of access of the reactant molecules into the internal pore structure and product diffusion limitations, and (iii) coke spreading over the external surface and direct coke formation on the external surface resulting in very low activity and reactor plugging by coke.

For pressures well into the supercritical regime, resulting in high reduced densities of the reaction mixture within the zeolite supercages (superdense phase, i.e., a fluid with a significantly higher density than that of the supercritical fluid in an empty reactor (24)), the supercritical reaction fluid *in situ* extracts the newly formed coke precursors through solubilization. Coke precursor solubilization occurs immediately after its formation. The dense supercritical fluid can also *in situ* extract the adsorbed olefinic products from the acid sites, reducing the probability for condensation and oligomerization reactions that result in coke formation. Therefore, heptane cracking under supercritical conditions should result in (i) smaller amounts of coke within the supercages and thus, a higher number of strongly acidic sites available for cracking, and (ii) a large number of unclogged pores and partially clogged pores, enabling the penetration of heptane in the supercages and reducing the diffusion limitations for the bulky reaction products and the dissolved coke precursors. Thus, the catalyst is stabilized toward severe and rapid deactivation.

Coke analysis results for subcritical and supercritical reaction conditions are shown in Table 4. The C/H ratio indicates that the coke formed under supercritical conditions has a different molecular structure than the coke formed under subcritical conditions, the latter being more graphitic (i.e., more aromatic). This was attributed to the fact that under subcritical conditions the coke molecules remain permanently in the supercages due to the low solubilization efficiency of the hydrocarbon and therefore, they undergo further condensation and dehydrogenation transformations. TGA results, shown in Fig. 4, are in excellent agreement with the above observation: Since coke is less graphitic under supercritical conditions, it burns at lower temperature as it is indicated by the position of the peak for the 4110 kPa experiment.

The most important aspect for the catalyst performance, however, is not the absolute amount of coke but the degree

TABLE 4

Coke Analysis Results for Supercritical ($P/P_c = 1.50$, $\rho_R = 1.40$) and Subcritical ($P/P_c = 0.62$, $\rho_R = 0.17$ and $P/P_c = 0.25$, $\rho_R = 0.09$) *n*-Heptane Catalytic Cracking at 475°C

P/P_c	Time (min)	%C	%H	C/H
1.50	300	6.05	1.11	5.45
1.03	300	8.08	0.86	9.39
0.25	40	6.50	0.83	7.83

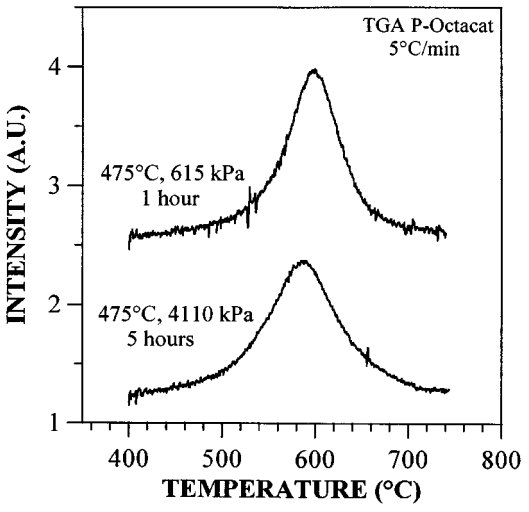

FIG. 4. TGA results for coke deposition on promoted Octacat after 5 h of *n*-heptane cracking under supercritical (4110 kPa, $\rho_R = 1.40$) conditions (bottom curve) and after 1 h of cracking under subcritical (615 kPa, $\rho_R = 0.09$) conditions (top curve).

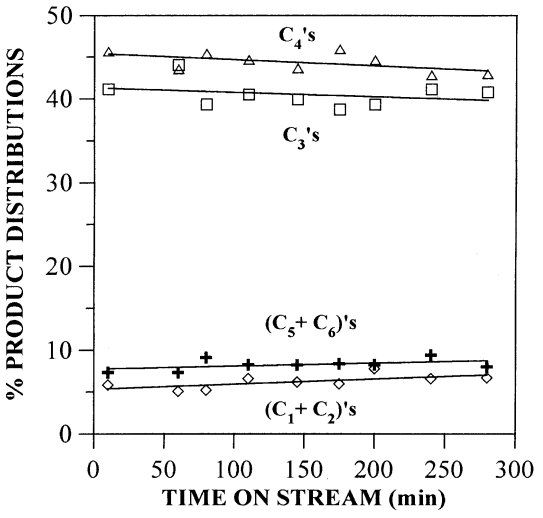

FIG. 6. Cracking product distribution at different times-on-stream for subcritical *n*-heptane catalytic cracking ($P/P_c = 0.62$, $\rho_R = 0.17$) at 475°C.

of obstruction of pore mouths. As mentioned before, *in situ* CIR-FTIR results (26) indicated that under subcritical conditions a significantly higher amount of coke was located on the external surface and therefore, a severe deactivation of the catalyst resulted by pore blockage.

Product Distribution and Reaction Mechanism

Changes in the product distributions (i.e., total C_2's, C_3's, C_4's, etc.) with time-on-stream are shown in Figs. 5 and 6. The cracking products consisted mostly of propane, propylene, C_4-paraffins, and olefins (linear and branched). Relatively small amounts of methane, ethane, and C_5–C_6 olefins were also present. C_5–C_6 paraffins were detected in small amounts only during the first 30 min of the reaction. Specifically at steady state, independent of the reaction pressure, $C_3 + C_4$ accounted for 84 mol% and $C_1 + C_2$ for 6.6%, and the balance was $C_5 + C_6$ of 9.4%. C_5 and C_6 cracking products were mainly linear while this was not the case for C_4's. We demonstrated that there was only a minor contribution from thermal cracking in all of the experiments carried out in this study. Experiments under identical reaction conditions using no catalyst showed that the total conversion for thermal cracking was less than 1%.

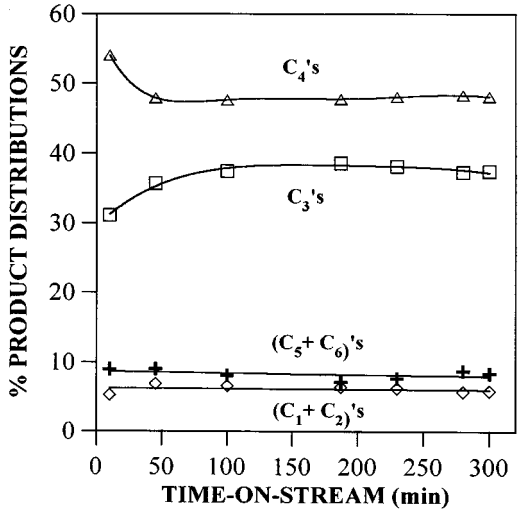

FIG. 5. Cracking product distribution at different times-on-stream for supercritical *n*-heptane catalytic cracking ($P/P_c = 1.50$, $\rho_R = 1.40$) at 475°C.

Of the primary products, propane was found to be the major cracking product followed by *n*-butane. On the other hand, propylene formation was favored by subcritical pressures and long times-on-stream. As these figures illustrate, supercritical reaction conditions favored the formation of C_4's relative to C_3's, especially at early reaction times.

In accord with the mechanism of paraffin cracking over zeolites shown in the scheme below at this temperature (31–34), propane and *n*-butane are major products in the *n*-heptane protolytic cracking (steps [2] and [3]) proceeding via formation of a nonclassical pentacoordinated carbonium ion, (n-$C_7H_{17}^+$) (step [1]), as transition state, and in the steps of hydride transfer from *n*-heptane to secondary propyl ($C_3H_7^+$) (step [12]) and butyl (n-$C_4H_9^+$) (step [13]) carbenium ions, respectively. Isobutane is formed by a hydride transfer from *n*-heptane to *tert*-butyl carbenium ion (i-$C_4H_9^+$) (step [6]). The latter is produced by isomerization of the secondary butyl carbenium ion which proceeds rapidly in comparison with the rate of *n*-heptane transformation (31), while isobutylene is formed from the desorption of the *tert*-butyl carbenium ion (step [11]).

The hydride transfer bimolecular reactions result in the formation of paraffins and n-C_7-carbenium ions (steps [12]–[14]). Furthermore, isomerization and β-scission of the

n-C_7-carbenium ions result in the formation of C_3^{2-} and C_4 (branched and linear, steps [17] and [19]), and C_3 and C_4^{2-} (branched and linear, steps [16] and [18]) fragments (19). This series of transformations is shown below:

Protolytic cracking

$$n\text{-}C_7H_{16} + H^+Z \leftrightarrow n\text{-}C_7H_{17}^+Z \text{ (transition state)} \quad [1]$$

$$n\text{-}C_7H_{17}^+Z \rightarrow C_3H_8 + n\text{-}C_4H_9^+Z \quad [2]$$

$$n\text{-}C_7H_{17}^+Z \rightarrow n\text{-}C_4H_{10} + C_3H_7^+Z \quad [3]$$

$$n\text{-}C_7H_{17}^+Z \rightarrow CH_4 + n\text{-}C_6H_{13}^+Z \text{ (small probability)} \quad [4]$$

$$n\text{-}C_7H_{17}^+Z \rightarrow C_2H_6 + n\text{-}C_5H_{11}^+Z \text{ (small probability)} \quad [5]$$

$$n\text{-}C_4H_9^+Z \leftrightarrow \text{i-}C_4H_9^+Z \quad [6]$$

$$n\text{-}C_4H_9^+Z \leftrightarrow 1\text{-}C_4H_8 + H^+Z \quad [7]$$

$$C_3H_7^+Z \leftrightarrow C_3H_6 + H^+Z \quad [8]$$

$$n\text{-}C_6H_{13}^+Z \leftrightarrow 1\text{-}C_6H_{12} + H^+Z \text{ (small probability)} \quad [9]$$

$$n\text{-}C_5H_{11}^+Z \leftrightarrow 1\text{-}C_5H_{10} + H^+Z \text{ (small probability)} \quad [10]$$

$$\text{i-}C_4H_9^+Z \leftrightarrow \text{i-}C_4H_8 + H^+Z \quad [11]$$

Hydride transfer bimolecular reactions

$$n\text{-}C_7H_{16} + C_3H_7^+Z \rightarrow C_3H_8 + n\text{-}C_7H_{15}^+Z \quad [12]$$

$$n\text{-}C_7H_{16} + n\text{-}C_4H_9^+Z \rightarrow n\text{-}C_4H_{10} + n\text{-}C_7H_{15}^+Z \quad [13]$$

$$n\text{-}C_7H_{16} + \text{i-}C_4H_9^+Z \rightarrow \text{i-}C_4H_{10} + n\text{-}C_7H_{15}^+Z \quad [14]$$

β-scission cracking mechanism

$$n\text{-}C_7H_{15}^+Z \leftrightarrow \text{i-}C_7H_{15}^+Z \quad [15]$$

$$n\text{-}C_7H_{15}^+Z \rightarrow 1\text{-}C_4H_8 + C_3H_7^+Z \quad [16]$$

$$n\text{-}C_7H_{15}^+Z \rightarrow C_3H_6 + n\text{-}C_4H_9^+Z \quad [17]$$

$$\text{i-}C_7H_{15}^+Z \rightarrow \text{i-}C_4H_8 + C_3H_7^+Z \quad [18]$$

$$\text{i-}C_7H_{15}^+Z \rightarrow C_3H_6 + \text{i-}C_4H_9^+Z \quad [19]$$

Coke formation (olefin oligomerization) reactions

$$C_mH_{2m} + C_nH_{2n+1}^+Z \rightarrow C_{m+n}H_{2(m+n)+1}^+Z \text{ (oligomer)} \quad [20a]$$

(olefin) (A_1S)

and/or

$$C_mH_{2m+1}^+Z + C_nH_{2n+1}^+Z \rightarrow C_{m+n}H_{2(m+n)+1}^+Z + H^+Z \quad [20b]$$

(A_1S)

Coke growth reactions

$$xC_pH_{2p} + C_{m+n}H_{2(m+n)+1}^+Z+ \rightarrow \text{Polymer} \quad [21]$$

(olefin) (A_2S)

$$\text{Polymer} \rightarrow \text{Coke.} \quad [22]$$

Polymerization is followed by cyclization, hydrogen transfer, alkylation, etc. (reaction [22]). The above protolytic cracking mechanism is responsible for the low formation of C_1 and C_2's (31) and also for the small amounts of C_6's and C_5's.

Figures 5 and 6 demonstrate that heptane cracking under subcritical conditions results in a lower C_4/C_3 ratio relative to the supercritical cracking. This is due to the severe blocking of the pores by coke laydown, which results in significant steric constraints for the diffusion of the bulkier C_4 products, especially the isobutane and isobutylene. This also explains the higher C_4/C_3 ratio for the supercritical experiment at short times-on-stream where the pore blocking was very limited.

Product Yields and Yield Ratios

Yield dependence. The changes in the total percentage yield for all detected products with time-on-stream are demonstrated in Fig. 7 while the steady-state lumped hydrocarbon product percentage yields are shown in Figs. 8 and 9 for paraffins and olefins, respectively. The percentage yield of a product p is defined as:

$$\%Y_p = \left(F_p/F_{\text{in}}^7\right) \times 100, \quad [23]$$

where F_p is the molar flow rate of product p, and F_{in}^7 is the heptane inlet molar flow rate. While yield data illustrate

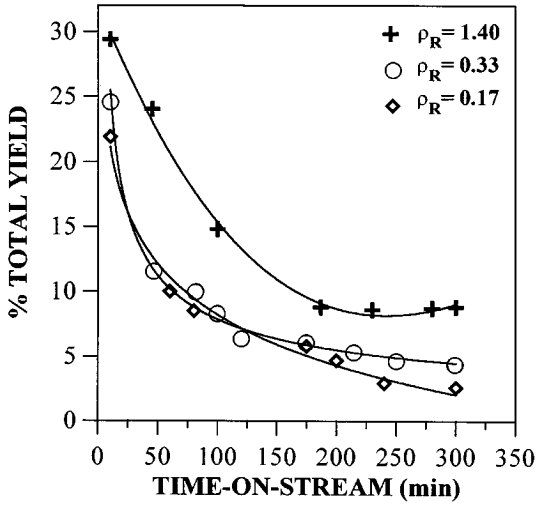

FIG. 7. Total percentage cracking product yield (excluding coke) at different times-on-stream for subcritical ($P/P_c = 0.62$, $\rho_R = 0.17$), near-supercritical ($P/P_c = 1.03$, $\rho_R = 0.33$), and supercritical ($P/P_c = 1.50$, $\rho_R = 1.40$) *n*-heptane catalytic cracking at 475°C.

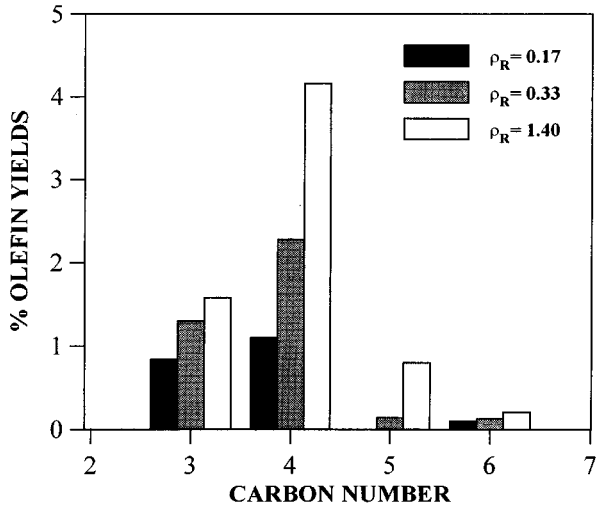

FIG. 8. Steady-state olefinic product percentage yields vs number of carbon atoms in the molecule for subcritical ($P/P_c = 0.62$, $\rho_R = 0.17$), near-supercritical ($P/P_c = 1.03$, $\rho_R = 0.33$), and supercritical ($P/P_c = 1.50$, $\rho_R = 1.40$) *n*-heptane catalytic cracking at 475°C.

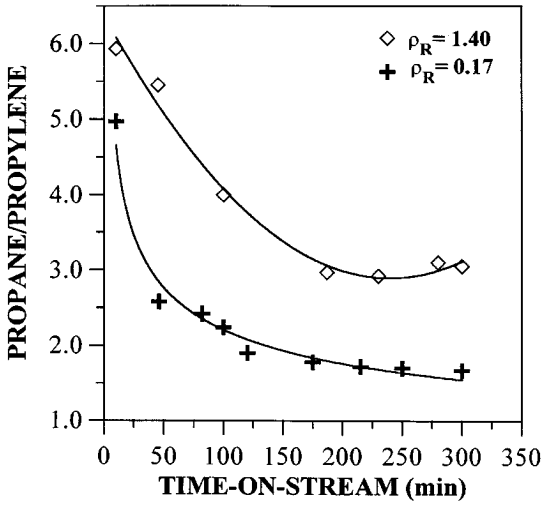

FIG. 10. C_3/C_3^{2-} yield ratios at different times-on-stream for *n*-heptane catalytic cracking at 475°C under subcritical ($\rho_R = 0.17$) and supercritical ($\rho_R = 1.40$) reaction conditions.

the activity status of the catalyst (i.e., higher yields indicate higher activity), yield ratios (equal to the ratios of the formation rates of products) offer information on the reaction mechanisms. Significantly higher steady-state yields for all major reaction products were obtained for the supercritical reaction, as a result of the lower catalyst deactivation. C_4 olefin and C_3 and C_4 paraffin yields were seriously affected by changes in pressure, the latter significantly increasing with increased pressure in the supercritical regime.

Paraffin to olefin ratio dependence. Figures 10 and 11 show the changes with time-on-stream for some paraffin/olefin yield ratios, and Fig. 12 shows branched/linear catalytic cracking products for two different experiments.

As these figures illustrate, the paraffin/olefin ratio depended strongly on operating pressure and reaction time. This ratio was always higher than 1.0 due to the rapid bimolecular hydride transfer reactions (reactions [12]–[14] in the above reaction scheme). This ratio, initially high, significantly decreased with time-on-stream, especially for the subcritical experiments, while for each reaction time it was substantially lower for subcritical pressures. This behavior can be explained on the basis of the existence of steric constraints in the partially and completely clogged pores of the zeolite by coke, which limit the bimolecular hydride

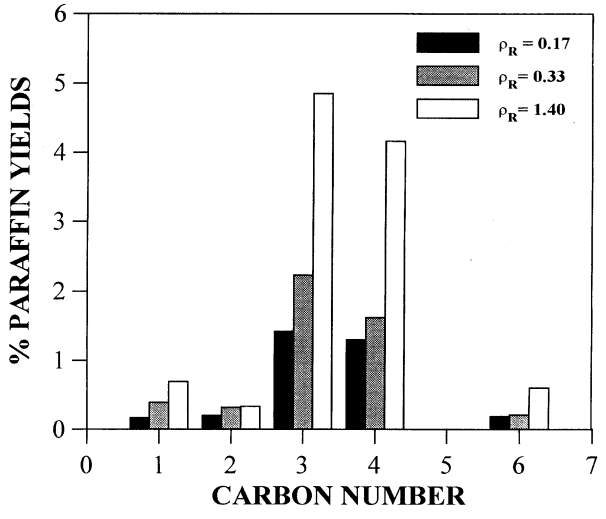

FIG. 9. Steady-state paraffinic product percentage yields vs number of carbon atoms in the molecule for subcritical ($P/P_c = 0.62$, $\rho_R = 0.17$), near-supercritical ($P/P_c = 1.03$, $\rho_R = 0.33$), and supercritical ($P/P_c = 1.50$, $\rho_R = 1.40$) *n*-heptane catalytic cracking at 475°C.

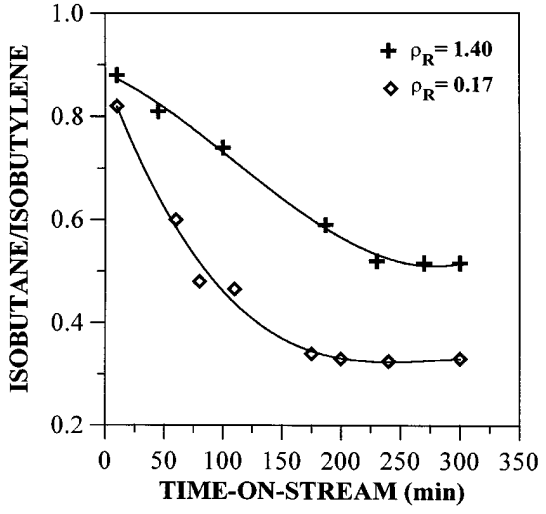

FIG. 11. $i\text{-}C_4^{2-}/i\text{-}C_4^{2-}$ yield ratios at different times-on-stream for *n*-heptane catalytic cracking at 475°C under subcritical ($\rho_R = 0.17$) and supercritical ($\rho_R = 1.40$) reaction conditions.

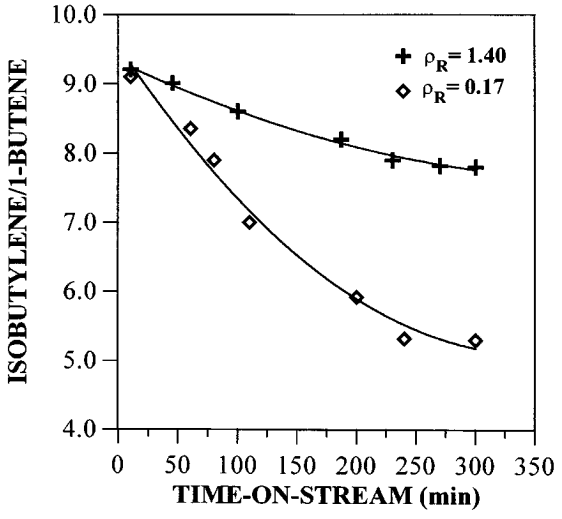

FIG. 12. i-C_4^{2-}/1-C_4^{2-} yield ratios at different times-on-stream for *n*-heptane catalytic cracking at 475°C under subcritical ($\rho_R = 0.17$) and supercritical ($\rho_R = 1.40$) reaction conditions.

transfer reactions (reactions [12]–[14]) when operating in the subcritical regime and/or at long times-on-stream. This is because the hydrogen transfer reactions proceed via a sterically large bimolecular transition state (31, 35).

According to Haag and Dessau (31), the cross section of the hydride transfer transition state is 4.9×6 Å^2 for the reaction between a secondary carbenium ion and *n*-hexane (reactions [12] and [13] in the scheme, where two secondary carbon atoms are involved in the reaction). On the other hand, the cross section of the transition state for the reaction between the tertiary butyl carbenium ion and *n*-hexane (reaction [14] in the scheme, where a secondary and a tertiary carbon atom are now involved) is 6×7 Å^2. This indicates that at short on-stream times, where little coke has formed and operation under supercritical conditions, where coke laydown is less than subcritical operation, the cracking catalyzed reactions involved both those of low steric constrains (reactions [1]–[11]) as well as higher steric crowding (reactions [12]–[14]) and subsequent reactions [15]–[19]. As the coke deposition increases at long on-stream times or operation under subcritical conditions, the cracking is dominated by reactions [1]–[11] and the ones of higher steric constrains [12]–[14] play a lesser role. This predicts that the C_3/C_3^{2-} ratio (shown in Fig. 10) and the *n*-C_4/1-C_4^{2-} ratio should be substantially higher at supercritical and short on-stream times. The i-C_4/i-C_4^{2-} ratio (shown in Fig. 11) should also be higher under the same conditions of operation. Figures 10 and 11 are in accord with these predictions as with the observed *n*-C_4/1-C_4^{2-} ratio, which was significantly higher.

Therefore, when operating in the regime of high coke deposition (subcritical and long times on stream), the catalyst operates mainly in the protolytic cracking reaction regime (reactions [1]–[10]), resulting in paraffin/olefin ratios close to 1.0, while for small coke to moderate coke laydown regimes it operates in both the protolytic cracking (reactions [1]–[10]) and hydride transfer, β-scission regimes (reactions [12]–[19]), resulting in high paraffin/olefin ratios.

Branched to linear ratio dependence. The high isobutylene/1-butene yield ratio under all operating conditions and reaction times, shown in Fig. 12, suggests that the butyl carbenium ion isomerization reaction (reaction [6]) is more favorable relative to the 1-butene formation reaction (reaction [7]). This was expected since the tertiary carbocation is more stable than the secondary. Under conditions of low coke formation (supercritical or low on-stream times) reactions [1]–[11] and [12]–[14] are both operative leading to a higher fraction of isomerized products, i.e., high isobutylene/1-butene ratios. Figure 12 shows this correlation.

Coke formation under supercritical and subcritical conditions. The carbon atom percentage coke yields (based on the total carbon atom mass balance) at different times-on-stream are shown in Fig. 13, while the carbon atom percentage coke selectivities are shown in Fig. 14 for subcritical and supercritical cracking conditions. When the catalyst is active (short on-stream times or supercritical conditions), maintaining a high concentration of active acid sites and producing high concentrations of surface adsorbed olefinic carbenium ions ($C_nH_{2n+1}^+Z$, $C_mH_{2m+1}^+Z$), it favors the olefin oligomerization reactions (mainly step [20]) resulting in higher coke production rates and therefore, higher coke yields. This accounts for the higher coke yields observed at steady state (220–300 min) for the supercritical experiment relative to the subcritical and for the fact that coke yield, in general, decreases with time-on-stream. This observation was not surprising, since coke is also a reaction product;

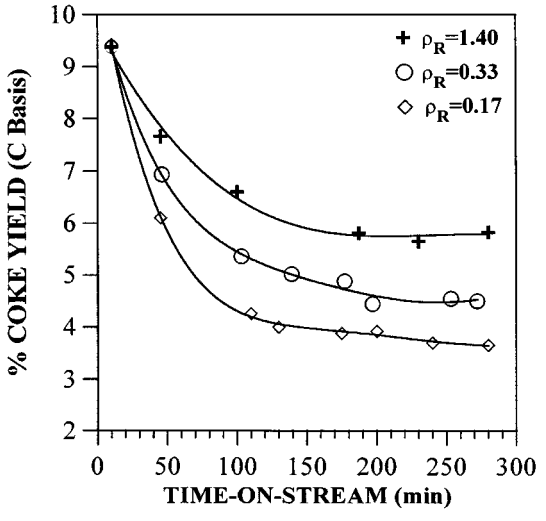

FIG. 13. Carbon atom percentage coke yields vs time-on-stream for *n*-heptane catalytic cracking at 475°C under subcritical ($\rho_R = 0.17$), near-supercritical ($\rho_R = 0.33$), and supercritical ($\rho_R = 1.40$) reaction conditions.

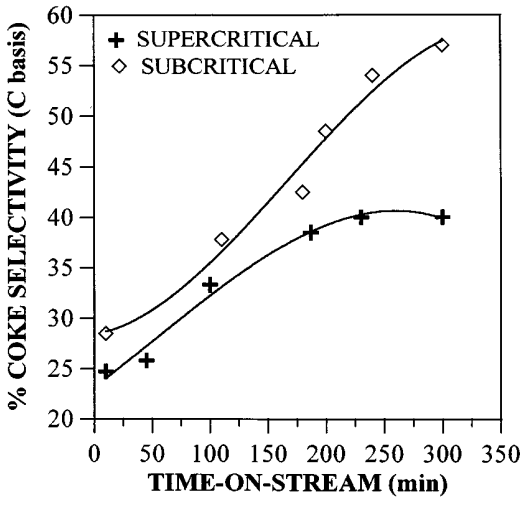

FIG. 14. Carbon atom percentage coke selectivities vs time-on-stream for *n*-heptane catalytic cracking at 475°C under subcritical ($\rho_R = 0.17$) and supercritical ($\rho_R = 1.40$) reaction conditions.

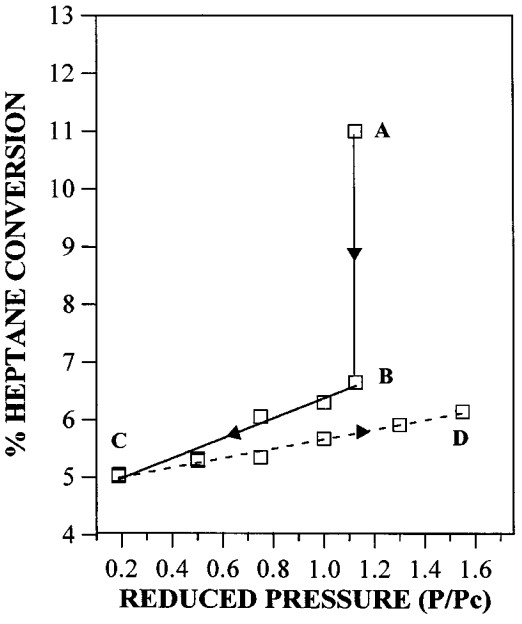

FIG. 15. Changes in the *n*-heptane conversion level with different pressures at 475°C for a severely deactivated cracking catalyst (promoted Octacat).

therefore, its yield follows the same functional trend with operating conditions and time-on-stream as the yields of all other cracking products. In other words, the coke yield under supercritical conditions is higher because the heptane conversion is higher.

Coke selectivity is a better index for analyzing the relative coke-making tendency of the catalyst. Low coke selectivity is an indicator of the tendency to produce less coke relative to the desired reaction products. As Fig. 14 illustrates, supercritical reaction conditions result in substantially lower coke selectivity relative to the subcritical conditions. The difference becomes more pronounced at long reaction times. This is because for subcritical cracking, diffusion limitations affect the migration of the olefins and especially of the bulky isobutylene (36, 19), when the catalyst is severely deactivated by pore plugging. Since these compounds diffuse out of the porous network of the zeolite more slowly, they rapidly undergo secondary transformations leading to further coke formation in the catalyst micropores (19).

The newly formed coke precursors (A_1S and A_2S) are *in situ* dissolved by the reaction fluid during supercritical heptane cracking. Indeed, the reactor effluent is black due to the fine coke particles. However, for the optimum operating pressure regime, if some coke precursors are not dissolved by the supercritical fluid they will grow into larger molecules, which are more difficult to extract. Therefore, complete avoidance of catalyst deactivation under supercritical conditions may not be possible unless the rate of precursor removal can be accelerated. Activity maintenance is achieved whenever the coke extraction rate equals the coke formation and coke buildup rates. At the highest ρ_R of 1.40, both the heptane conversion (Fig. 1) and coke yield (Fig. 13) reach a constant, steady-state activity.

Catalyst regeneration by supercritical fluids. To answer the question whether a catalyst that had been deactivated under subcritical cracking conditions could be reactivated by simply switching back to supercritical reaction conditions several experiments shown in Figs. 15 and 16 were

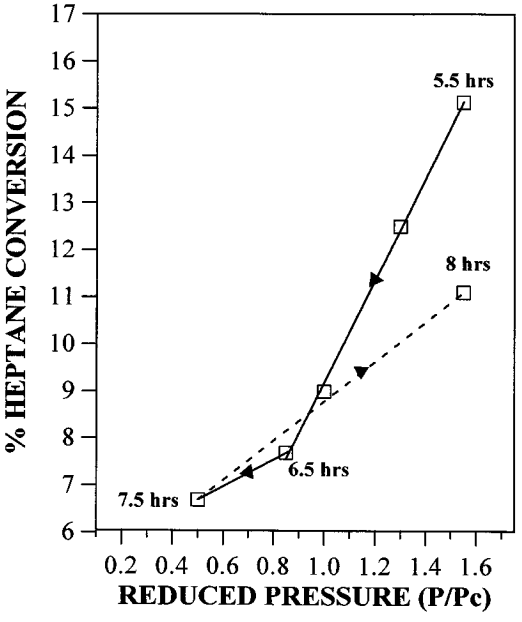

FIG. 16. Changes in the *n*-heptane conversion level with different pressures at 475°C for a catalyst (promoted Octacat) moderately deactivated after 5 h of *n*-heptane cracking under supercritical conditions ($P/P_c = 1.50$, $\rho_R = 1.40$).

carried out. In Fig. 15, after 5 h of reaction at 2850 kPa ($P/P_c = 1.03$, $\rho_R = 0.33$) (point A), the heptane flow rate was stopped for half an hour in order for the catalyst to be severely deactivated due to the gradual decrease in pressure. Then the system was filled up again with heptane at 2850 kPa and the heptane conversion was substantially reduced as expected (point B). Gradually decreasing the pressure well into the subcritical regime over a period of 2 h (from B to C) did not further deactivate the catalyst. On the other hand, when the pressure was again increased from subcritical to supercritical values over a 2-h time period, the heptane conversion level practically did not increase. These data show that the supercritical fluid cannot regenerate a severely deactivated catalyst.

However, for moderately deactivated catalyst, Fig. 16 shows that reactivation is possible. For this experiment, the pressure after 5 h of reaction under high pressure ($P/P_c = 1.50$, $\rho_R = 1.40$) was gradually decreased to subcritical values, with a subsequent decrease in the conversion level. *In situ* CIR-FTIR spectra (26) showed a significant reduction in the number of active sites accompanying the decrease in the conversion level. When the pressure was increased back to 4110 kPa ($\rho_R = 1.40$) an increase in the conversion was observed but the recovery of the catalyst was not complete, since the original conversion was 16% and the final conversion, shown in Fig. 16, was 11%. *In situ* infrared spectra analysis (26) also showed that the concentration of the active sites was again increased. Therefore, it was demonstrated that supercritical heptane was able only to partially dissolve the extra coke that was formed under the less severe subcritical reaction conditions, in agreement with the conclusions of Manos and Hoffman (13).

The above findings are consistent with the following mechanism: The pore structure of promoted Octacat includes micropores, mesopores, and zeolitic pores within the commercially formulated kaolin-Y-type matrix. When the catalyst is fresh and active, high cracking rates to olefins result. This also leads to a high rate of formation of surface-bound oligomers and coke. As previously reported (21), the coke grows inside of the supercage and out through the pore mouths into the much longer mesopores in the kaolin matrix. Our infrared results support that this coke growth and deposition is outside the zeolite pore since the terminal silanol bands rapidly decreased in intensity as coke deposition increased (26). Within the zeolitic pore, where the supercritical heptane is at its highest density, the hydrocarbon can continuously remove both oligomers and severe coke growth sites. This regeneration of strong Brønsted acid cracking sites under supercritical operation was clearly demonstrated by the infrared study (26). However, any degree of coke deposition within the pores and pore mouths result in a diffusion restriction for products. This is especially detrimental to olefin production since this leads to a higher residence time within the supercage and results in their conversion to coke. Operation in the supercritical regime results in the continuous removal of coke from the zeolite pores and results in a relatively high steady-state activity. When coke deposition is very high as in operation at subcritical, a large fraction of coke spills over to the mesopores of the kaolin matrix. Here the density of heptane is much lower; consequently, the supercritical heptane within these large pores cannot extract coke as fast as it is formed. Then total activity loss results and it cannot be totally recovered by operation in the supercritical regime. For these reasons we conclude that supercritical heptane should not be able to completely regenerate a severely deactivated catalyst. The extent of the partial catalyst regeneration by a supercritical fluid should depend on its deactivation history, i.e., the operating temperature, pressure, and time-on-stream.

CONCLUSIONS

Kinetic measurements of *n*-heptane catalytic cracking over a commercial Y-type zeolite (promoted Octacat) at 475°C under supercritical and subcritical conditions showed that the catalyst maintained a substantially higher activity when operated under heptane pressures well into the supercritical regime. The stabilization of the catalyst toward rapid deactivation was primarily attributed to the continuous removal of the coke (deposited on the catalytic sites in the zeolite supercages, pore mouths, and external surface) through solubilization by the supercritical heptane. Coke extraction under the studied supercritical reaction conditions resulted in a higher number of available active sites in the supercages and in less pore diffusion restrictions for both reactant and products due to the avoidance of pore blockage. The significant increase in the steady-state yields of all reaction products for supercritical cracking can also be explained by the above mechanism. Finally, it was shown that only a partial regeneration of a moderately deactivated cracking catalyst is possible by the supercritical reaction medium. Reactivation of a severely deactivated catalyst by the supercritical fluid was not possible.

ACKNOWLEDGMENTS

The authors acknowledge the Air Force Office of Scientific Research for financial support of this study under Grant Contract AFOSR G: F49620-93-1-0204. The contribution and collaboration of the United Technologies Research Center in this research project is also gratefully acknowledged.

REFERENCES

1. Lang, X., Akgerman, A., and Bukur, D., *Ind. Eng. Chem. Res.* **34**, 72 (1995).
2. Savage, P. E., Gopalan, S., Mizan, T. I., Martino, C. J., and Brock, E. E., *AIChE J.* **41**(7), 1723 (1995).
3. Tiltscher, H., Wolf, H., and Schelchhorn, J., *Angew. Chem. Int. Ed.* **20**, 892 (1981).

4. Tiltscher, H., Wolf, H., and Schelchhorn, J., *Ber. Bunsenges, Phys. Chem*. **88**, 897 (1984).
5. Tiltscher, H., and Hoffman, H., *Chem. Eng. Sci.* **45**, 5 (1987).
6. Subramaniam, B., and McHugh, M. A., *Ind. Eng. Chem. Process Des. Res.* **25**, 1 (1986).
7. Saim, S., and Subramaniam, B., *J. Supercrit. Fluids* **3**, 214 (1990).
8. Saim, S., and Subramaniam, B., *J. Catal.* **131**, 445 (1991).
9. Baptist-Nguyen, S., and Subramaniam, B., *AIChE J.* **38**(7), 1027 (1992).
10. Subramaniam, B., and McCoy, B. J., *Ind. Eng. Chem. Res.* **33**, 504 (1994).
11. Ginosar, D. M., and Subramaniam, B., *J. Catal.* **152**, 31 (1995).
12. Yokota, K., and Fujimoto, K., *Ind. Eng. Chem. Res.* **30**, 95 (1991).
13. Manos, G., and Hoffman, H., *Chem. Eng. Technol.* **14**, 73 (1991).
14. Jolly, S., Saussey, J., and Lavalley, J. C., *J. Mol. Catal.* **86**, 401 (1994).
15. Chaar, M. A., and Butt, J. B., *Appl. Catal. A: General* **114**, 287 (1994).
16. Pinheiro, C. I., Lemos, F., Ramoa Ribeiro, F., and Guisnet, M., *Appl. Catal. A: General* **108**, 107 (1994).
17. Lopes, J. M., Lemos, F., Ramoa Ribeiro, F., Derouane, E. G., Magnoux, P., and Guisnet, M., *Appl. Catal. A: General* **114**, 161 (1994).
18. Meusinger, J., Liers, J., Mosch, A., and Reschetilowski, W., *J. Catal.* **148**, 30 (1994).
19. Magnoux, P., Guisnet, M., Mignard, S., and Cartraud, P., *J. Catal.* **117**, 495 (1989).
20. Mignard, S., Cartraud, P., Magnoux, P., and Guisnet, M., *J. Catal.* **117**, 503 (1989).
21. Magnoux, P., Cartraud, P., Mignard, S., and Guisnet, M., *J. Catal.* **106**, 242 (1987).
22. Reid, R. C., Prausnitz, J. M., and Poling, B. E., "The Properties of Gases and Liquids," 4th ed., pp. 36–39. McGraw-Hill, 1987.
23. Spadaccini, L. J., Colket, M. B., and Marteney, P. J., *in* "Proceedings, JANNAF Populsion Meeting, October 1990."
24. Dardas, Z., Süer, M. G., Ma, Y. H., and Moser, W. R., *J. Catal.* **159**, 204 (1996).
25. Peng, D. Y., and Robinson, D. B., *Ind. Eng. Chem. Fundam.* **15**, 59 (1976).
26. Süer, M. G., Dardas, Z., Ma, Y. H., and Moser, W. R., *J. Catal.*, in press.
27. Brennecke, J. F., and Eckert, C. A., *J. Phys. Chem.* **94**, 7692 (1990).
28. Petche, I., and Debenedetti, P. G., *J. Phys. Chem.* **91**, 7075 (1989).
29. Chialvo, A. A., and Debenedetti, P. G., *Ind. Eng. Chem. Res.* **31**, 1391 (1992).
30. Dardas, Z., Suer, M. G., Ma, Y. H., and Moser, W. R., *in* "Proceedings, Catalysis Society of New England, December 1994."
31. Haag, W. O., and Dessau, R. M., *in* "Proceedings, 8th International Congress on Catalysis, Berlin, 1984," Vol. 2, p. 305. Dechema, Frankfurt-am-Main, 1984.
32. Corma, A., Planelles, J., Sanchez-Marin, J., and Tomas, F., *J. Catal.* **93**, 30 (1985).
33. Lukyanov, D. B., *J. Catal.* **147**, 494 (1994).
34. Zhao, Y., Bamwenda, G. R., and Wojciechowski, B. W., *J. Catal.* **146**, 594 (1994).
35. Chen, N. Y., and Haag, W. O., *in* "Hydrogen Effects in Catalysis: Fundamentals and Practical Applications" (Z. Paal and P. G. Menon, Eds.), p. 695. Dekker, New York, 1988.
36. Mirodatos, C., and Bartomeuf, D., *J. Catal.* **93**, 246 (1985); **114**, 121 (1988).